Processing STIM-LAB's experimental data on slot flow of proppants

Part I
D.D. Joseph, and Jimmy Wang
University of Minnesota

Part II
Neelesh Patankar
Northwestern University

February 2001

Table of contents

Part I

STIM-LAB carried out two types of experiments looking at the transport of proppants in thin fluids. The first experiment can be described as a lift-off experiment. A somewhat simplified description of the experiment is that a bed of proppant is eroded by the flow of water. Proppant is not injected. The faster the flow of water the deeper is the channel above. We are seeking to predict the height above the channel. The experiment is described in Appendix 1. Of particular relevance is their data Table 4.9.4.9-1. This data table described the condition called "channelized flow" in section 4.9.2.2. The channel width is 0.8cm in all experiments. The density and size of proppants and the water temperature is given in Table 4.9.4.1-1. The water temperature controls the viscosity.

The second experiment (Appendix 2) is different than the first because proppant plus fluid is continuously injected. If the inflow rates are fixed the system reaches a steady state as is described in "Modeling 4-6" in which proppant is transported as a moving, mildly inflated porous bed, called a "mobile bed," below a fully fluidized suspension called a traction carpet. If we look away from the ends of the eight-foot long by one-foot tall by 3/16" wide channel, the flow of proppants and liquid is fully developed as in the diagram shown in our Figure 1 below.

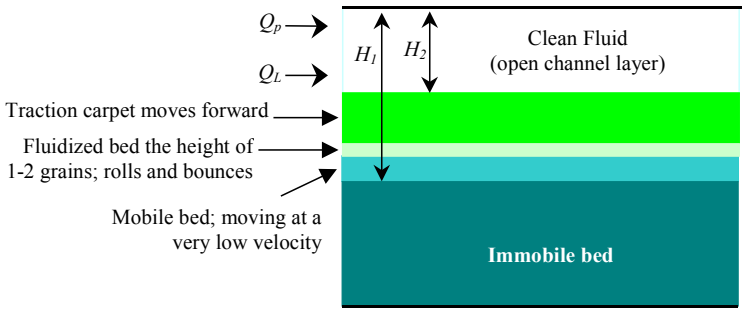

Figure 1. Proppant flowing in a channel.

Nomenclature

ρ_p density of the particles, gm/cm^3
d mean diameter of the particles, cm
ρ_f density of the fluid, gm/cm^3
η dynamic viscosity of the fluid, gm/cm-s
$\overline{p}$ average pressure gradient applied in the flow direction (if available), gm/(cm-s)^2
Q_f volumetric flow rate of the fluid, cm^3/s
M_p mass flow rate of the proppants, gm/s
Q_p volumetric flow rate of the proppants = M_p/ρ_p, cm3/s
Q_T total volumetric flow rate (fluid + proppant) = $Q_f + Q_p$, cm^3/s
h open channel height cm; (H_2)
H_1 see Figure 1, cm
H_2 see Figure 1, cm
W channel width 0.79375cm
A area cc; ($A = W * H_2$)

υ kinematic viscosity c^2/s; $\upsilon = \dfrac{\eta}{\rho_f}$

V fluid velocity cm/s; $V = \dfrac{Q}{A} = \dfrac{Q}{WH_2}$;

$\widetilde{V}$ fluid velocity cm/s; $\widetilde{V} = \dfrac{Q}{W^2}$;

R Reynolds number (based on V); $R = \dfrac{Vd}{\upsilon}$;

$\widetilde{R}$ Reynolds number (based on $\widetilde{V}$); $\widetilde{R} = \dfrac{\widetilde{V}d}{\upsilon} = \dfrac{RH_2}{W}$;

G gravity parameter; $G = \dfrac{(\rho_p - \rho_f)gd^2}{\eta V}$;

R_G gravity Reynolds number; $R_G = \dfrac{\rho_f(\rho_p - \rho_f)gd^3}{\eta^2} = GR$;

S Shields parameter is defined as: $S = \dfrac{\tau}{(\rho_p - \rho_f)gd}$;

If we take $\tau = \eta\dot{\gamma}_w$ and $V = \dot{\gamma}_w d$, then $S = \dfrac{\eta V}{(\rho_p - \rho_f)gd^2} = \dfrac{1}{G}$.

Scaling parameters

In the paper *Lift Correlations from Direct Numerical Simulation of Solid-Liquid Flows* (Joseph 2001) we found scaling parameters for the flow of particles in fluids for simulations in two dimensions. The two most important were a Reynolds number for the forward flow

$$R = Vd/\eta \tag{1}$$

and a sedimentation "Reynolds number" based on the settling velocity $\frac{\rho_f(\rho_p - \rho_f)gd^2}{\eta}$ in Stokes flow.

$$R_G = \rho_f \frac{(\rho_p - \rho_f)gd^3}{\eta^2} \tag{2}$$

The fluid velocity V is related to the pressure drop across the flow cell.

It is important to do correlations in terms of dimensionless parameters; this leads to maximum generality. To see this consider power laws, which we found, that are of the form

$$R_G = aR^n \tag{3}$$

for lift-off. For R larger than $(R_G)^{1/n}/a$, the particle of radius d and density ρ_p will levitate. This equation (3) may be written as

$$\rho_f \frac{(\rho_p - \rho_f)gd^3}{\eta^2} = a\left(\frac{Vd}{\eta}\right)^n \tag{4}$$

Suppose we did experiments for lift-off in a certain fluid with a given proppant of different size. We would find a correlation of the form

$$V = bd^m \tag{5}$$

We wouldn't know that $m = {}^3/_n - 1$ or how all the other parameters enter into the correlation.

Erosion experiments; for these experiments $H_1 = H_2$ and only water is moving.

STIM-LAB did experiments on bed erosion. These are essentially lift-off experiments since the flow rate is dropped to a critical lift-off value below which particles are not eroded from the bed.

In Table 1 we reformulate the data from tables 4.9.4.9-1 and 4.9.4.1-1 in Appendix 1 for processing in terms of R_G and

$$\widetilde{R} = \frac{\widetilde{V}d}{\nu} \tag{6}$$

where

$$\widetilde{V} = \frac{Q}{W^2} \tag{7}$$

and Q is the volume flow rate. We use $\widetilde{V}$ because Q and W are prescribed data.

There are seven groups in the data shown in Table 1; each one corresponds to a value of R_G. The data corresponding to a given R_G is ordered by increasing H_2; the larger R corresponds to a larger H_2 more or less, but there are exceptions.

Proppants	d (cm)	H_2 (cm)	η (gm/cm•s)	ρ_f (gm/cc)	υ (cm^2/s)	Q (cc/s)	ρ_p (gm/cc)	R_G	$\tilde{V}$ (cm/s)	$\tilde{R}$	H_2/W
60/40 Brady	0.034212	1.7	0.01115	0.999	0.011161	36.778	2.65	521.1645	58.37416	178.9337	2.141732
	0.034212	2.3	0.01115	0.999	0.011161	58.289	2.65	521.1645	92.51649	283.5899	2.897638
	0.034212	5.6	0.01115	0.999	0.011161	133.295	2.65	521.1645	211.5662	648.512	7.055118
	0.034212	7.8	0.01115	0.999	0.011161	232.588	2.65	521.1645	369.1644	1131.596	9.826772
20/40 Ottawa	0.056043	2.3	0.01115	0.999	0.011161	46.556	2.65	2290.822	73.89383	371.0382	2.897638
	0.056043	5.2	0.01115	0.999	0.011161	133.106	2.65	2290.822	211.2663	1060.817	6.551181
	0.056043	8.2	0.01115	0.999	0.011161	227.542	2.65	2290.822	361.1554	1813.446	10.33071
20/40 Light Beads	0.06	1.4	0.01115	0.999	0.011161	7.885	1.05	86.83778	12.5151	67.27847	1.76378
	0.06	2	0.01115	0.999	0.011161	10.409	1.05	86.83778	16.5212	88.8144	2.519685
	0.06	3.9	0.01115	0.999	0.011161	31.92	1.05	86.83778	50.66353	272.3562	4.913386
	0.06	8.5	0.01115	0.999	0.011161	128.438	1.05	86.83778	203.8572	1095.892	10.70866
	0.06	12	0.01115	0.999	0.011161	226.217	1.05	86.83778	359.0523	1930.188	15.11811
16/20 Carbolite	0.094946	1.5	0.01	0.998	0.01002	31.542	2.73	14513.72	50.06356	474.3833	1.889764
	0.094946	2.2	0.01	0.998	0.01002	50.467	2.73	14513.72	80.10138	759.0103	2.771654
	0.094946	9.9	0.01	0.998	0.01002	258.642	2.73	14513.72	410.5174	3889.907	12.47244
16/20 Carbolite	0.094946	1.7	0.00378	0.972	0.003889	36.778	2.73	100415.8	58.37416	1425.188	2.141732
	0.094946	2.3	0.00378	0.972	0.003889	58.289	2.73	100415.8	92.51649	2258.763	2.897638
	0.094946	5.6	0.00378	0.972	0.003889	133.295	2.73	100415.8	211.5662	5165.329	7.055118
	0.094946	7.8	0.00378	0.972	0.003889	232.588	2.73	100415.8	369.1644	9013.043	9.826772
16/30 Banrite	0.088437	0.4	0.01115	0.999	0.011161	10.535	3.45	13363.76	16.72119	132.4925	0.503937
	0.088437	0.6	0.01115	0.999	0.011161	13.878	3.45	13363.76	22.02721	174.5354	0.755906
	0.088437	1.3	0.01115	0.999	0.011161	29.145	3.45	13363.76	46.25904	366.5394	1.637795
	0.088437	3.5	0.01115	0.999	0.011161	100.681	3.45	13363.76	159.8012	1266.205	4.409449
	0.088437	8.3	0.01115	0.999	0.011161	261.796	3.45	13363.76	415.5234	3292.454	10.45669
12/20 Badger	0.109021	1.3	0.01015	0.998	0.01017	28.955	2.65	20342.9	45.95747	492.643	1.637795
	0.109021	2.5	0.01015	0.998	0.01017	62.137	2.65	20342.9	98.62404	1057.205	3.149606
	0.109021	5.8	0.01015	0.998	0.01017	155.185	2.65	20342.9	246.3101	2640.332	7.307087
	0.109021	9	0.01015	0.998	0.01017	290.814	2.65	20342.9	461.5809	4947.936	11.33858

Table 1: Data set for lift-off experiments from Table 4.9.4.9-1 in Appendix 2

Power fit: H_2/W *vs.* $\tilde{R}$ *in a log-log plot*

It is rather obvious that the height H_2 will increase with Q at a fixed R_G (for fixed proppant and fluid). With R_G fixed we can hope for a two-parameter correlation. In Figure 2 we show seven more or less straight lines for the seven values of R_G. The power law for these is given by

$$\frac{H_2}{W} = a(R_G)\, R^{m(R_G)} \tag{8}$$

where $a(R_G)$ and $m(R_G)$ are listed in Table 2. The value of the exponent $m(R_G) \approx 0.87$ for all cases except $R_G = 86.84$ corresponding to nearly neutrally buoyant particles ($\rho_p = 1.05$ gm/cc).

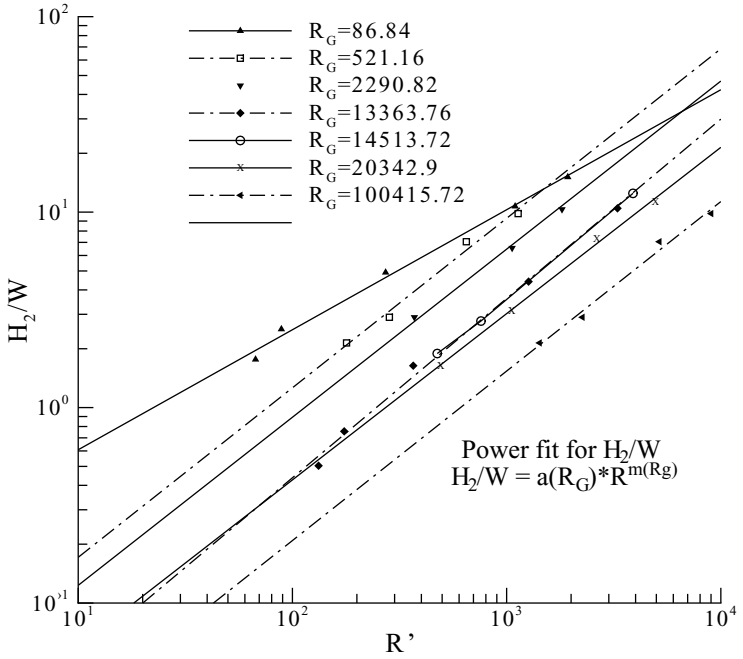

Figure 2. H_2/W *vs.* $\widetilde{R}$ *in log-log plot for different values of* R_G *(see Table 2).*

R_G	$a(R_G)$	$m(R_G)$
86.84	1.479E-1	0.6140
521.16	2.326E-2	0.8672
2290.822	1.700E-2	0.8600
13363.76	6.393E-3	0.9174
14513.72	6.40E-3	0.9170
20342.90	8.476E-3	0.8508
100415.72	3.847E-3	0.8672

Table 2. The coefficients (as functions of R_G*) used in power fit for* H_2/W.

Inspection of Table 2 shows that when $R_G \geq 521$

$$m(R_G) \approx 0.87 \tag{9}$$

whereas when $R_G = 86.84$ ($\rho_p = 1.05$) we get

$$m(R_G) \approx 0.61\ . \tag{10}$$

This shows that the exponent m does depend on and we may hope to describe this dependence in intervals (as is true for the Richardson-Zaki $n(R)$, which depends in intervals on the Reynolds number R). For example, we could suppose that there is a certain value of $R_G = R_{GC}$ for which the $m(R_G)$ take on the two values, (9) if $R_G > R_{GC}$ and (10) is $R_G < R_{GC}$ where $86.84 \leq R_{GC} \leq 521.16$.

Summarizing we may propose

$$\frac{H_2}{W} = a(R_G)\, R^{m(R_G)} \tag{11}$$

where $m(R_G)$ are given approximately by (9) and (10).

The final correlation $\mathbf{a(R_G)}$ *as* $\mathbf{R_G}$ *in a log-log plot*

We plotted $a(R_G)$ as given in Table 2 against R_G in a log-log plot. This plot is shown in Figure 3 and gives rise to the formula

$$a = 0.8007\, R_G^{\,-0.4854} \tag{12}$$

For the coefficient $a(R_G)$

$$a(R_G) = b \times R^k{}_G$$

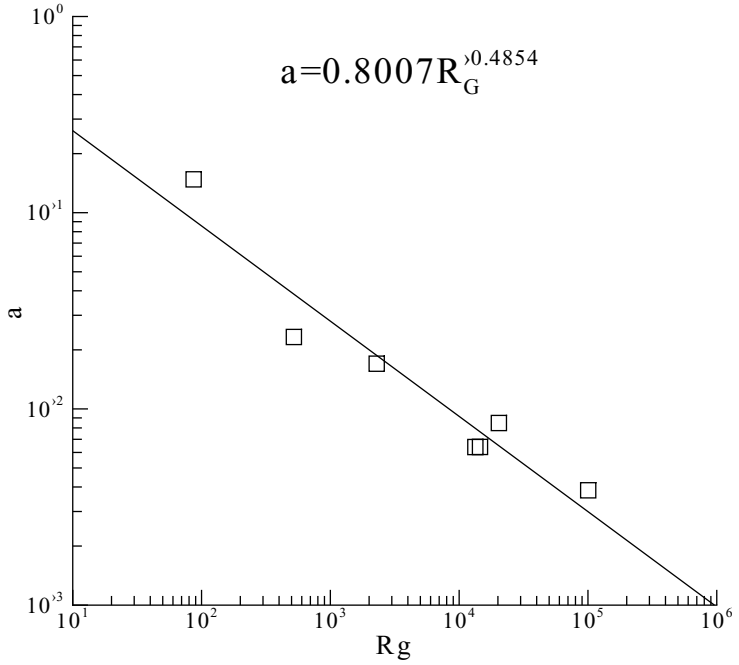

Figure 3. Power fit for $\mathrm{a(R_G)}$ *vs.* $\mathrm{R_G}$.

Combining now (11) and (12)

$$\frac{H_2}{W} = 0.8007 \times R_G^{-0.4854} \times \widetilde{R}^{m(R_G)} \tag{13}$$

where $m(R_G) \approx 0.87$ for $R_G > R_{GC}$, where $86 < R_{GC} < 500$ and $m \approx 0.614$ for $R_G < R_{GC}$.

We are proposing (13) as a widely applicable correlation for lift-off valid beyond where data has already been taken. More experiments, testing (13) validity for different values of W under more extreme conditions ought to be undertaken; of particular interest are light particles for which $R_G < R_{GC}$.

When $R_G > R_{GC}$ we can write (13) as

$$\frac{H_2}{W} = 0.8007\left[\frac{\rho_f(\rho_p - \rho_f)gd^3}{\eta^2}\right]^{-0.4854}\left(\frac{\rho_f Qd}{W^2\eta}\right)^{0.87} \tag{14}$$

Equation (14) gives the fracture height in terms of given quantities. Formula (13) can be expressed in terms of the Shield's parameter $1/G$ by writing $\widetilde{R} = \frac{R_G H_2}{GW}$.

Correlations for "channelized flow" (see Figure 1) with continuous slurry injection

Tables 3 and 4 prepare the data taken from Table 4.9.4.1-1 for processing in log-log plots. In Figure 4 we plotted H_2 (the height of the open channel) again the proppant rate Q_p in a log-log plot for Ottawa sand and in Figure 5 we do the same for Carbolite. These plots give rise to straight lines corresponding to power laws of the form

$$H_2 = aQ_p^n \tag{15}$$

where Q_f/Q is nearly the same on each straight line but differs from line to line.

H_1	H_2	Q_p	Q_f	Q	Q_p/Q	Q_f/Q
2.3	0.8	40	244.1	284.1	0.140795	0.859205
2.6	0.7	45.7	242.9	288.6	0.158351	0.841649
2.3	1	28.6	250.4	279	0.102509	0.897491
2.4	1.5	11.4	249.8	261.2	0.043645	0.956355
3	2.1	11.4	313.5	324.9	0.035088	0.964912
2.9	1.5	34.3	304.7	339	0.10118	0.89882
3.1	2.3	11.4	314.8	326.2	0.034948	0.965052
3	1.4	45.7	303.4	349.1	0.130908	0.869092
3	1.5	40	305.3	345.3	0.115841	0.884159
2.9	1.6	28.6	306	334.6	0.085475	0.914525
2.8	1.7	22.8	306	328.8	0.069343	0.930657
3.1	2	17.1	315.4	332.5	0.051429	0.948571
3.5	2.9	5.7	314.2	319.9	0.017818	0.982182
4.1	3.6	2.9	313.5	316.4	0.009166	0.990834
5.1	5	1.4	312.9	314.3	0.004454	0.995546
5.8	5.7	0.4	311.6	312	0.001282	0.998718

*Table 3. Parameters associated with the channeling experiment for **Ottowa** in Figure 1.*

H_1	H_2	Q_p	Q_f	Q	Q_p/Q	Q_f/Q
2	1.2	11.2	180.4	191.6	0.058455	0.941545
2.1	1.2	16.8	180.4	197.2	0.085193	0.914807
1.7	0.5	22.3	180.4	202.7	0.110015	0.889985
1.9	0.6	27.9	180.4	208.3	0.133941	0.866059
1.9	0.4	33.5	180.4	213.9	0.156615	0.843385
1.7	0.2	44.7	180.4	225.1	0.198578	0.801422
2.4	1.5	5.6	192.4	198	0.028283	0.971717
2.8	2.1	2.8	193.7	196.5	0.014249	0.985751
3	2.8	1.4	193.7	195.1	0.007176	0.992824
3.3	2.8	0.7	195.6	196.3	0.003566	0.996434
4.3	3.9	0.3	195.6	195.9	0.001531	0.998469
2.9	1.6	22.3	306.6	328.9	0.067802	0.932198
2.9	2	11.2	307.2	318.4	0.035176	0.964824
3.3	2.6	5.6	306	311.6	0.017972	0.982028
4	3.2	2.8	309.7	312.5	0.00896	0.99104
4	3.2	1.4	311	312.4	0.004481	0.995519
4.2	3.5	0.7	311	311.7	0.002246	0.997754
5.3	5	0.3	316	316.3	0.000948	0.999052
3.1	1	44.7	315.4	360.1	0.124132	0.875868
3	1.2	39.1	314.2	353.3	0.110671	0.889329
3	1.3	33.5	308.5	342	0.097953	0.902047
3	1.3	27.9	310.5	338.4	0.082447	0.917553
2.9	1.6	22.3	309.1	331.4	0.06729	0.93271
3	1.8	16.8	312.1	328.9	0.051079	0.948921
3.2	2.1	11.2	318.6	329.8	0.03396	0.96604
3.4	2.6	5.6	321.1	326.7	0.017141	0.982859
3.5	2.9	4.2	316	320.2	0.013117	0.986883

*Table 4. Parameters associated with the channeling experiment for **Carbolite** in Figure 1.*

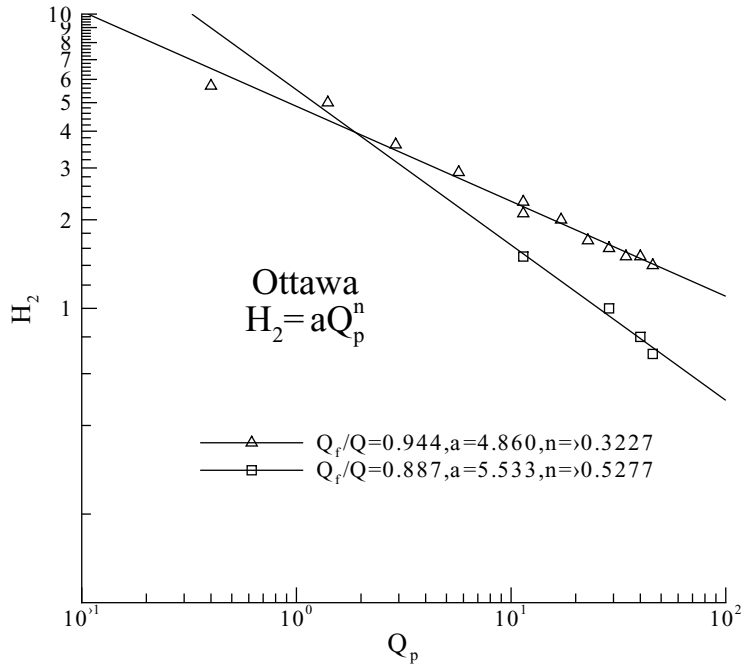

Figure 4. H_2 *vs.* Q_p *for Ottawa (see table 3). This correlation is not framed between dimensionless variables, but the lines are pretty straight.*

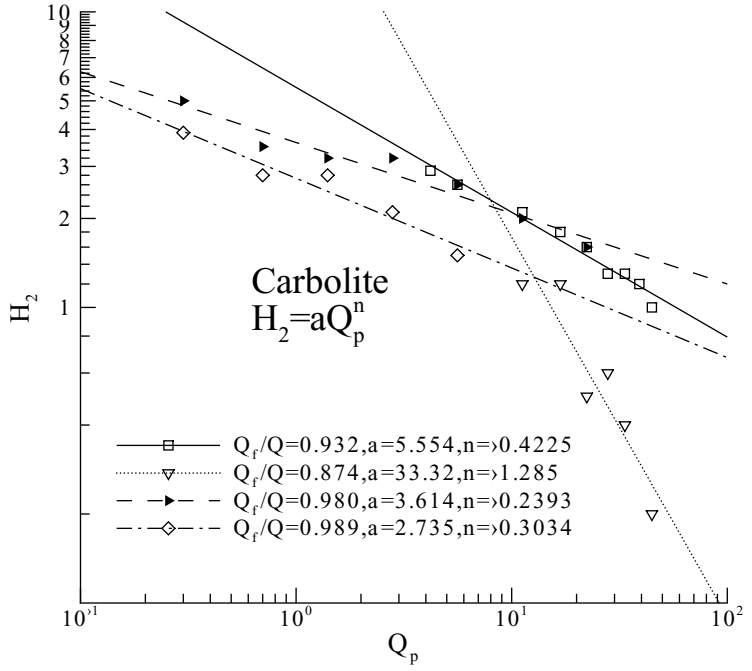

Figure 5. H_2 *vs.* Q_p *for Carbolite (see table 4). Straight lines describe the data well.*

Correlations for

$$a(Q_f/Q) \quad \text{and} \quad n(Q_f/Q)$$

are obtained from the 6 mean values of Q_f/Q listed in Table 5. These correlations are shown in Figures 6 and 7.

H_1	H_2	Q_p	Q_f	Q	Q_p/Q	Q_f/Q
3.53	2.61	18.48	310.11	328.58	0.056	0.94
2.4	1	31.43	246.8	278.23	0.11	0.89
3.16	2.62	2.16	194.2	196.36	0.011	0.99
3.8	3.01	6.33	309.64	315.97	0.02	0.98
3.12	1.76	22.81	313.94	336.76	0.068	0.93
1.88	0.68	26.07	180.4	206.47	0.13	0.87

Table 5. Mean values of H_1, H_2, Q_p, Q_f, Q, Q_p /Q, Q_f /Q. *These mean values are used for the* "a" *and* "n" *correlations in Figures 6 and 7.*

Power fit for the coefficient *a* were tried by using:

$$a = b(Q_f/Q)^m \tag{16}$$

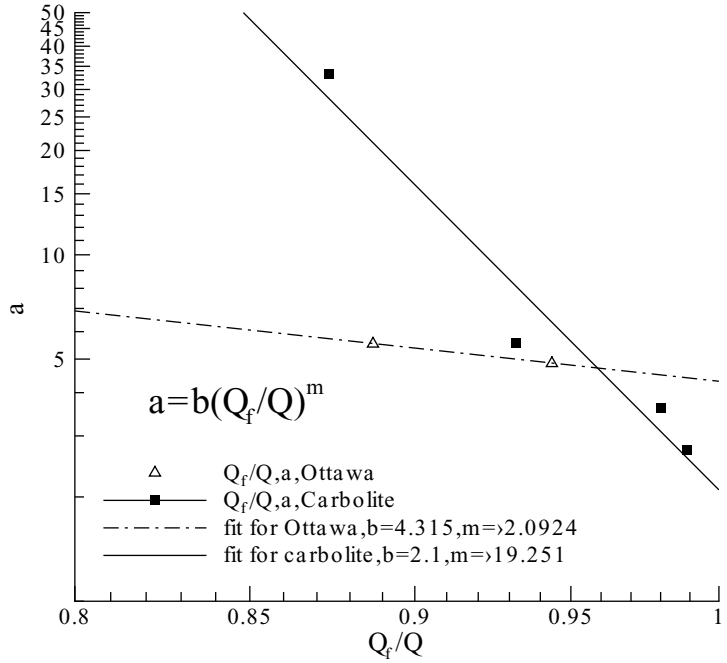

Figure 6. Fit for coefficient a *with* Q_f/Q. *The* "a" *correlation for Carbolite is not perfect.*

Power fit for the coefficient *n* were tried by using:

$$-n = c(Q_f/Q)^k \tag{17}$$

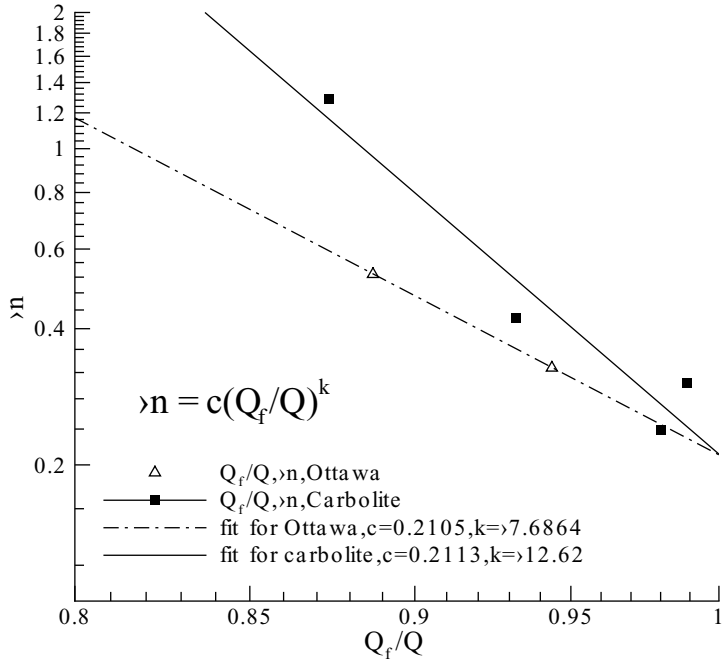

Figure 7. Fit for coefficient n *with* Q_f/Q.

Combining now (15), (16) and (17) we get the final dimensional correlation:

$$H_2 = b(Q_f/Q)^m (Q_p)^{-c(Q_f/Q)^k} \tag{18}$$

where

For Ottawa, $b = 4.315$, $m = -2.0914$; $c = 0.2105$, $k = -7.6864$;

For Carbolite, $b = 2.1$, $m = -19.251$; $c = 0.2113$, $k = -12.62$

Dimensionless correlation

A dimensionless correlation

$$\frac{H_2}{W} = a\left(\frac{Q_p}{Q}\right)^n \tag{19}$$

is presented in Figures 8 through 11. The correlations for Ottawa and Carbolite are satisfactory.

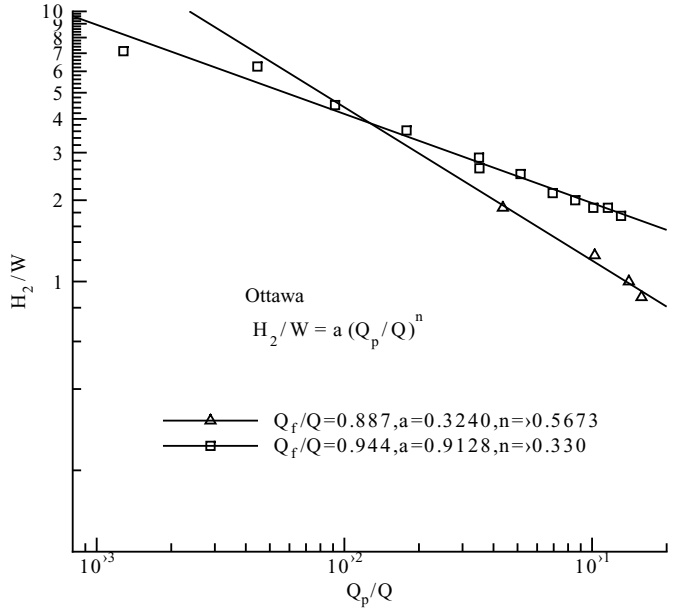

Figure 8. H_2/W *vs.* Q_p/Q *for Ottawa (see table 3).*

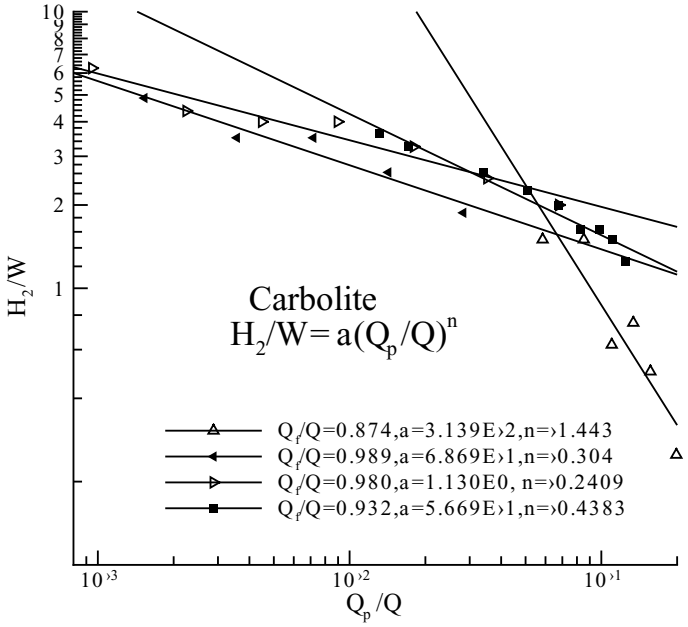

Figure 9. H_2 *vs.* Q_p/Q *for Carbolite (see table 4).*

Logically a and n in the correlation should depend on the fluid rate fraction Q_f/Q. A power fit

$$a = b(Q_f/Q)^m \tag{20}$$

is given in Figure 10.

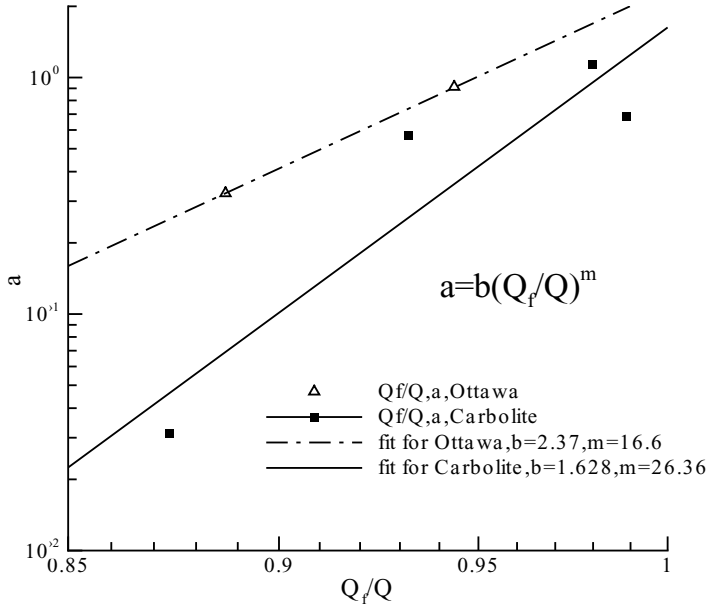

Figure 10. Fit for coefficient a *with* Q_f/Q.

A power fit for the exponent n

$$-n = c(Q_f/Q)^k. \tag{21}$$

is given in Figure 11.

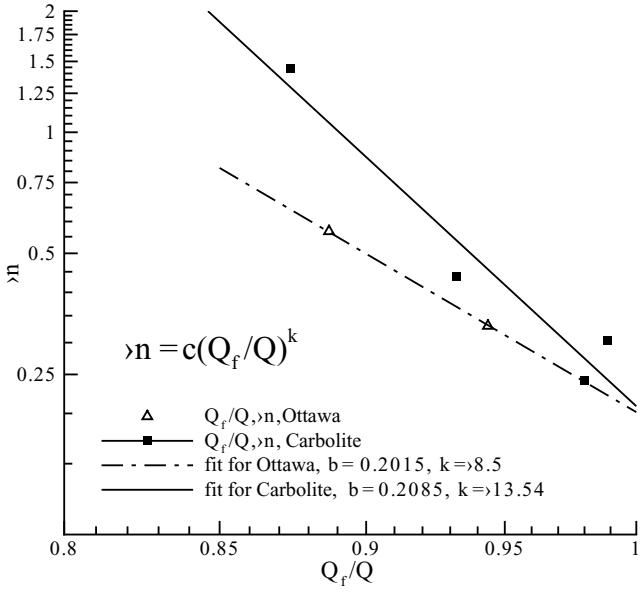

Figure 11. Fit for coefficient n *with* Q_f/Q.

The fit for "a" and "n" in Figures 10 and 11 are not very good. Putting together (19), (20) and (21) we get

$$H_2/W = b(Q_f/Q)^m (Q_p/Q)^{-c(Q_f/Q)^k} \qquad (22)$$

where

For Ottawa, b = 1.92, m = 16.71; c = 0.2015, k = -8.5.

For Carbolite, b = 1.303, m = 26.36; c = 0.2085, k = -13.54.

The bedload correlations just developed lack generality since they are not expressed in terms of the basic parameters, the Reynolds numbers R and R_G. In the next section Neelesh Patankar will look at this more general problem.

Part II

Power law correlation for bed load transport

Neelesh A. Patankar

Northwestern University

Variables:

ρ_p	density of the particles, gm/cm^3
d	mean diameter of the particles, cm
ρ_f	density of the fluid, gm/cm^3
η	dynamic viscosity of the fluid, gm/cm-s
$\overline{p}$	average pressure gradient applied in the flow direction (if available), gm/(cm-s)^2
Q_f	volumetric flow rate of the fluid, cm^3/s
M_p	mass flow rate of the proppants, gm/s
Q_p	volumetric flow rate of the proppants = M_p/ρ_p, cm^3/s
Q_T	total volumetric flow rate (fluid + proppant) = $Q_f + Q_p$, cm^3/s
H_1	see Figure 1, cm
H_2	see Figure 1, cm
W	width of the channel, cm

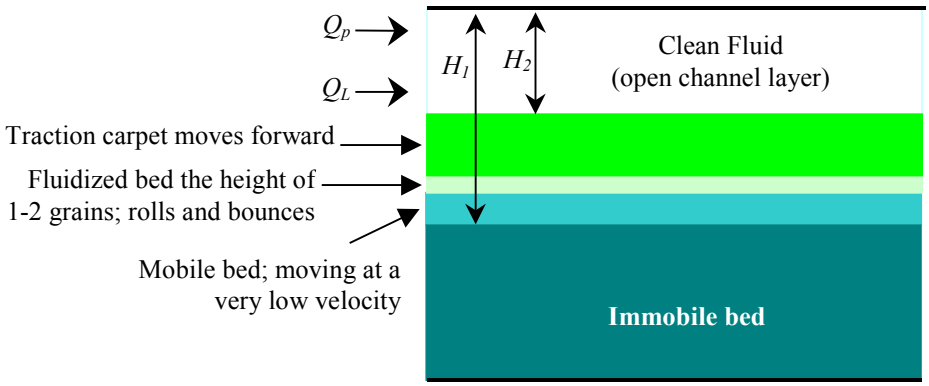

Figure 1. Proppant flowing in a channel

Data set 1: $H_1 = H_2 = H$

Define a Reynolds number $R_q = \dfrac{\rho_f Q_f}{W\eta}$. Figure 2 shows a plot of R_q vs. H/W at different values of R_G where $R_G = \dfrac{981\rho_f\left(\rho_p - \rho_f\right)d^3}{\eta^2}$.

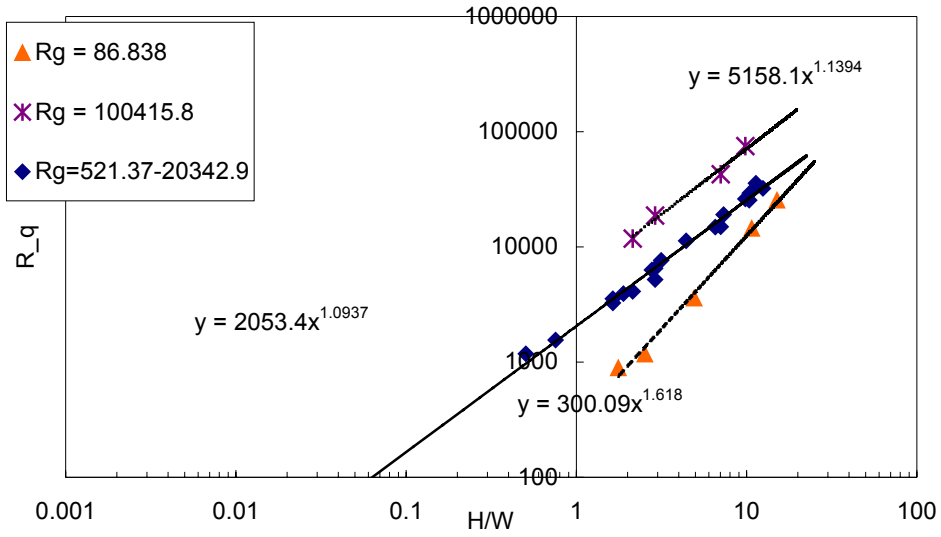

Figure 2. Plot (log-log) of R_q *vs.* H/W *at different values of* R_G.

We get

$$R_q = a(H/W)^n, \tag{1}$$

where *a* and *n* are function of R_G. We see that *a* and *n* may be regarded to be constant for $521.37 \le R_G \le 20342.9$. More experimental data will be required to obtain a smooth equations for *a* and *n* as functions of R_G. The values we have are plotted in Figures 3(a) and 3(b).

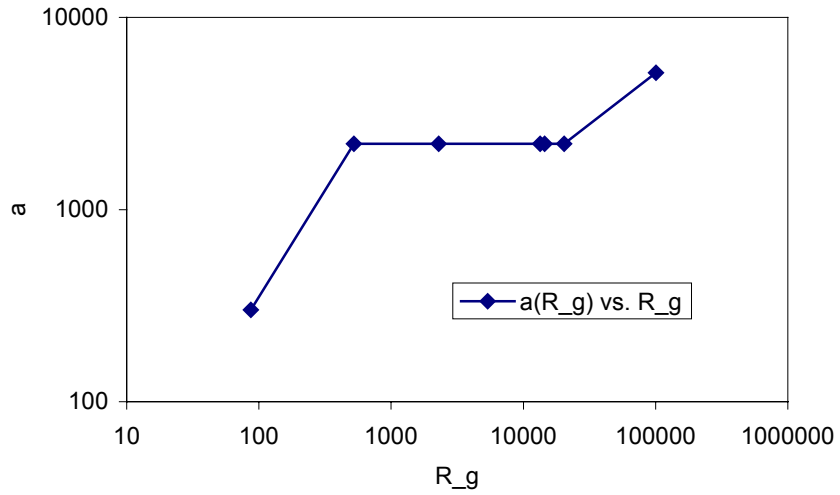

Figure 3(a). Plot (log-log) of a *vs.* R_G.

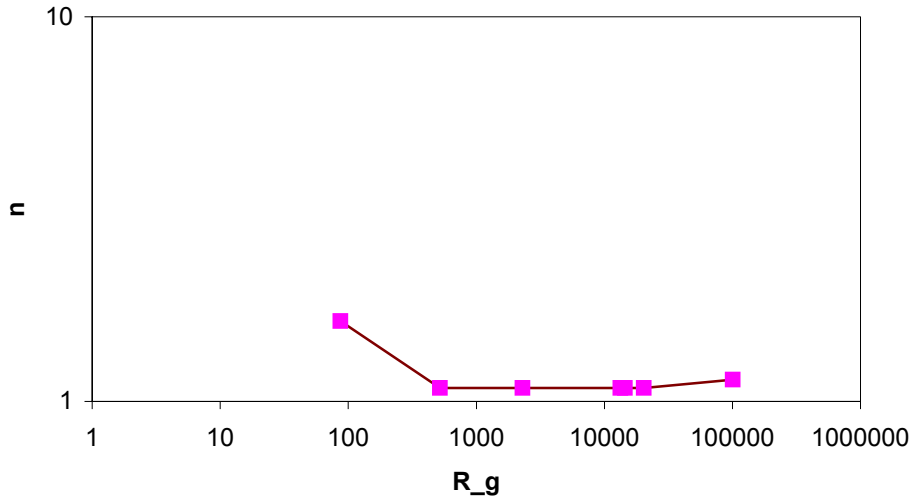

Figure 3(b). Plot (log-log) of n *vs.* R_G.

The data above represents the critical condition for the bed to start moving. We define an effective Reynolds number at the fluid bed interface as

$$R_{eff} = R_q(W/H)^n, \tag{2}$$

where the values of *n* are given in Figure 2 and plotted in Figure 3.

From the above plots we can write an expression for the critical effective Reynolds number R_{eff}^{cr} for bed motion as

$$R_{eff}^{cr} = a(R_G) \tag{3}$$

Data set 2: $H_1 \neq H_2$

Correlation for the fluid flow rate

We have two cases: 1. Carbolite: R_G = 12229 and 2. Ottawa: R_G = 3496. From the above correlation we see that

$$R_{eff}^{cr} = 2053.4 \tag{4}$$

Define the effective Reynolds number at the fluid bed-load interface as $R_{eff} = R_q(W/H_2)^{1.0937}$ for the Carbolite and Ottawa data.

Figure 4 shows a plot of R_{eff} vs. $\ln(H_1/H_2)$ for the combined Carbolite and Ottawa data.

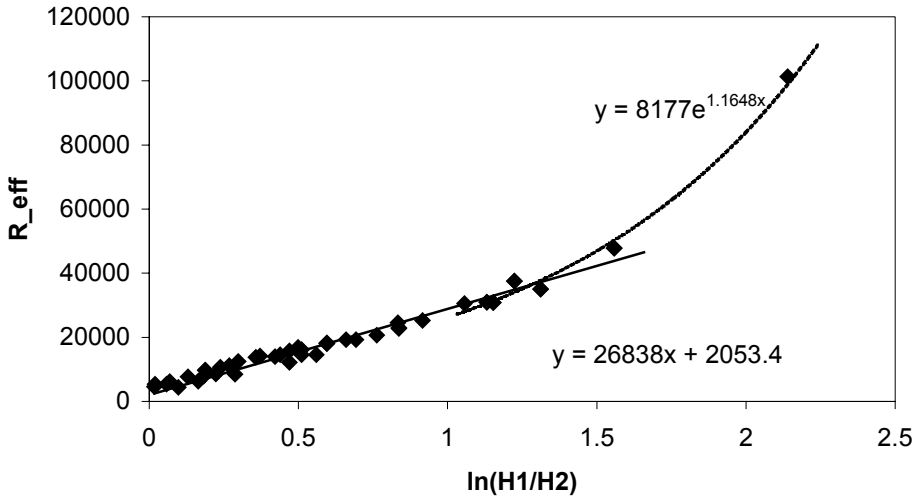

Figure 4. Plot of R_{eff} *vs. ln(*H_1/H_2*) for the combined Carbolite and Ottawa data.*

Two regimes are observed for the given values of R_G:

$$1.\ R_{eff} - R_{eff}^{cr} = 26838\ln(H_1/H_2);\ \ln(H_1/H_2) \le 1.3. \tag{5}$$

$$2.\ R_{eff} = 8177(H_1/H_2)^{1.1648};\ \ln(H_1/H_2) > 1.3. \tag{6}$$

Note that the y-intercept is taken to be equal to R_{eff}^{cr}. Regime 1 shows logarithmic behavior whereas regime 2 shows power law behavior. When $H_1/H_2 = 1$, we recover the correlation in (3). Thus (5) represents a combined correlation from the data set 1 and 2. Lastly, regimes 1 and two have an overlap region. Hence $\ln(H_1/H_2) = 1.3$ is only an approximate value for transition.

The correlation can be rewritten as:

$$\left(\frac{\rho_f Q_f}{H_2 \eta}\right)(W/H_2)^{n-1} - a(R_G) = 26838\ln(H_1/H_2);\ \ln(H_1/H_2) \le 1.3 \tag{7}$$

and

$$\left(\frac{\rho_f Q_f}{H_2 \eta}\right)(W/H_2)^{n-1} = 8177(H_1/H_2)^{1.1648};\ \ln(H_1/H_2) > 1.3. \tag{8}$$

Note that more data is required to obtain a complete correlation especially in the power law regime. Currently, only part of the Carbolite data lies in the power law regime. Ottawa data lies completely in the logarithmic regime.

Equations (5) and (6) can be represented by a single equation given by (Bob Baree, private communication)

$$R_{eff} = \frac{8177\left(H_1 / H_2\right)^{1.1648}}{\left(1+\left(\frac{H_1 / H_2}{0.9}\right)^{-9}\right)^{5}} \tag{9}$$

Model for bed load transport The above correlation suggests the following model for bed-load transport.

Consider a channel with a given height H_2 and width W. Begin the fluid flow in the channel. After a critical value Q_f, given by (2), the fluid begins to move the proppant in the bed. The height H_2 remains the same but the depth H_1-H_2 increases as the fluid flow rate is increased. The depth H_1 to which the bed moves can be found from (7). This is regime 1 or the bed erosion regime.

The correlation suggests a logarithmic behavior in regime 1 given by

$$dR_{eff} = -m\frac{dH}{H} \tag{10}$$

Integrating we get

$$\begin{aligned} \int_{R_{eff}^{cr}}^{R_{eff}} dR_{eff} &= -\int_{H_1}^{H_2} m\frac{dH}{H} \\ R_{eff} - \mathrm{Re}_{eff}^{cr} &= m\ln\left(\frac{H_1}{H_2}\right) \end{aligned} \tag{11}$$

A theoretical model to explain this equation may be constructed, details of which are not included here.

The depth H_1 increases up to a certain value (in this case corresponding to $\ln(H_1/H_2) \sim 1.3$). Further increase in the fluid flow rate does not increase H_1, hence the bed begins to 'inflate' or 'expand'. This situation is identical to our numerical simulations. Bed expansion now causes the value of H_2 to decrease. This is regime 2 or the bed expansion regime. As expected from our numerical simulation results, we observe power law behavior in this regime.

Correlation for proppant flow rate

We need another correlation for the proppant flow rate. It is shown in Figure 5. Define a non-dimensional variable R_p for proppant flow rate as $R_p = \frac{\rho_f Q_p}{H_1 \eta}$.

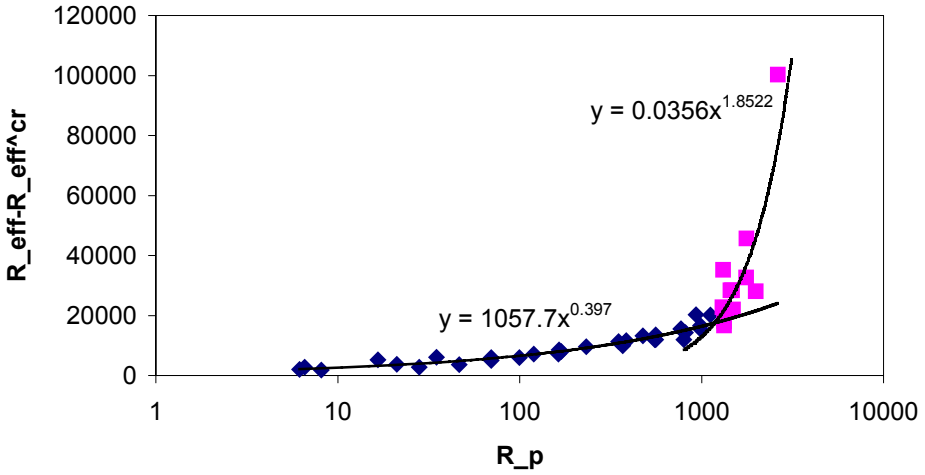

Figure 5. Plot (regular-log) of $R_{eff} - R_{eff}^{cr}$ *vs.* R_p.

Once again we observe two regimes. The correlations can be written as

$$\text{Regime 1 (Bed erosion):} \quad R_{eff} - R_{eff}^{cr} = 1057.7 R_p^{0.397} \tag{12}$$

$$\text{Regime 2 (Bed expansion):} \quad R_{eff} - R_{eff}^{cr} = 0.0356\, R_p^{1.8522} \tag{13}$$

Equations (12) and (13) can be represented by a single equation given by (Bob Baree, private communication)

$$R_{eff} - R_{eff}^{cr} = \frac{1057.7 R_p^{0.397}}{\left(1 + \left(\frac{R_p}{1185.07}\right)^5\right)^{-0.291}} \tag{14}$$

Conclusion: Correlations obtained are given by (3), (5)-(6) (or (9)) and (12)-(13) (or (14)).